CrystEngComm

Accepted Manuscript

ROYAL SOCIETY OF CHEMISTRY

www.rsc.org/crystengcomm

Journal Name

RSCPublishing

COMMUNICATION

Towards understanding P-gp resistance: a case study of the antitumour drug cabazitaxel

Cite this: DOI: 10.1039/xoxxooooox

U. Baisch[ab] and L. Vella-Zarb*[ab]

Received ooth January 2012,
Accepted ooth January 2012

DOI: 10.1039/xoxxooooox

www.rsc.org/

A detailed structural study and Hirshfeld surface analysis of cabazitaxel in its anhydrous, hydrated and solvated forms has revealed that the three-dimensional architecture of the drug molecule is retained regardless of crystalline environment. This prompted comparison with its taxane predecessors, suggesting key factors contributing to cabazitaxel's poor affinity to P-gp.

Classified as potent anticancer agents, the taxanes paclitaxel and docetaxel exert their antineoplastic action by stabilizing microtubules, thus leading to blockage of mitosis and eventually cell death[1,2]. They are used as first line treatment in a variety of cancers including ovarian, lung, head, neck and prostate, among others[3,4]. In spite of their widespread use, their efficacy is greatly hindered by their affinity for multidrug-resistance proteins[5], in particular P-glycoprotein (P-gp), an ATP-dependent drug efflux pump[6]. As resistance to taxanes is brought about by expression of P-gp by cancer cells[7], there have been increased attempts at synthesizing taxane analogs that are not P-gp substrates. Cabazitaxel, a semisynthetic taxane that was approved by the FDA in 2010[8], has poor affinity for P-gp, and has been found to be successful as second line treatment in docetaxel-resistance cancers such as advanced prostate cancer and castration-resistant prostate cancer among others[9-14].

Since paclitaxel, docetaxel and cabazitaxel molecules all consist of a taxane core with various side-chains attached to it, differences in binding affinity and membrane permeation have so far been attributed to the different polar substituents (Fig. 1) found on the core. However, a recent study of the structure of P-gp suggested that most residues that constitute the drug-binding site on this protein are in fact non-polar[15], inspiring thought about whether the lack of hydroxyl groups on cabazitaxel is really the only factor responsible for its success in evading multidrug-resistance proteins. Although many hypotheses exist as to the nature of this difference in affinity, there is a lack of literature available, whether experimental or theoretical, that deals with the three-dimensional architecture of these taxanes. The reasons for this could be difficulty in obtaining single crystals of suitable size, the actual size of the molecules, or the disorder that is observed in some of these structures. This knowledge gap prompted us to carry out a series of single crystal synchrotron and variable temperature laboratory powder X-ray diffraction experiments in an effort to understand the solid state behaviour of cabazitaxel compared to its predecessors, providing crystallographic evidence for its different protein-binding tendencies. A number of cabazitaxel hydrates and solvates were characterized in addition to the taxane in its anhydrous form, and their arrangement and structural conformations were analysed and compared in order to identify the important structural differences that exist between the newer-generation drug and its predecessors. We were also able to differentiate between the structural attributes that are a result of the crystallization process and those that are intrinsic to the molecule and thus retained in all the various forms.

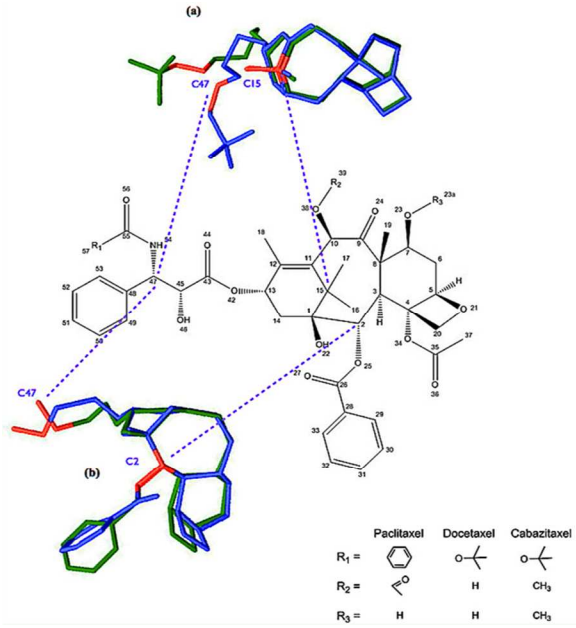

Fig. 1 Taxane anticancer drug molecules paclitaxel, docetaxel and cabazitaxel. Enlarged three-dimensional inserts show superimposed fragments of cabazitaxel (green) and docetaxel (blue) to highlight conformational differences in improper torsion angle (a) C17-C15···C47-N54 and (b) O25-C2···C47-N54. Origins of torsion are depicted in red.

Structural analyses of paclitaxel[16], docetaxel[17] and cabazitaxel reveal marked differences in the three-dimensional arrangement of their side-chains in the anhydrous forms, while solvates and hydrates of all three showed comparable features. We believe that the reason for cabazitaxel's success in circumventing P-gp binding, and possibly also its success in crossing the blood-brain barrier, may be attributable in part to its unique structural arrangement when compared to other taxanes.

When describing molecular conformation derived from crystal structures, it is very important to consider the effect of intermolecular interactions that might alter the conformation of the molecule significantly as a result of crystallization. Solvent molecules play an important role in the crystallisation of taxanes, providing a strong external influence upon the intermolecular interactions within the crystal. The intermolecular interactions between solvent molecule and taxane are usually the strongest ones in the crystal structure. Through our thorough study involving various solvates and hydrates as well as the anhydrous form of cabazitaxel, we present statistical and numerical evidence for the extreme flexibility of the side chain, and demonstrate that small changes in the molecular environment can affect its orientation greatly.

In spite of the two additional carbons present in cabazitaxel, its effective molecular volume is smaller than that of docetaxel or paclitaxel (ESI Table S1). The special orientation of the side chain exerts some influence on the molecular volume, making the molecule particularly small, folded, and non-polar on the surface. This might provide an explanation to cabazitaxel's higher success in overcoming binding to multidrug-resistance proteins when compared with docetaxel. Calculation of the Hirshfeld surfaces[18] of the three anhydrous forms revealed that curvedness and shape index, which are close to identical in the two early-generation taxanes, differ in cabazitaxel (ESI Table S1). This is demonstrated in Figure 2a, which illustrates the shape index of the molecular surface for each of the three forms. In the curvedness plots of docetaxel and paclitaxel there are large areas where the surface is flattened (Figure 2b), enabling π - π interactions with neighbouring molecules. This is not the case in cabazitaxel, which has a higher degree of curvedness as observed by the blue regions on the plot.

The difference in size is also highlighted on comparison of the global surface area of the fingerprint plots of the three taxanes extended to a d_e/d_i of 3Å (Figure 2c), which reveals that while cabazitaxel reaches 100%, paclitaxel and docetaxel cover 99.8% and 98.7% respectively. $H_{(int)}$ to $H_{(ext)}$ interactions are represented by the centre spike on the same plot, as highlighted in Figure 2d. This is much more pronounced in paclitaxel and docetaxel, reaching minimum distances $d_e + d_i$ of 1.4Å and 1.2Å respectively as opposed to 2.2Å in cabazitaxel. The same holds for $O_{(int)}$ to $H_{(ext)}$ interactions as minimum distances $d_e + d_i$ for paclitaxel, docetaxel and cabazitaxel reach 1.8Å, 1.6Å and 1.9Å respectively. These are denoted by the side spikes highlighted in Figure 2e, and while they are clearly more prominent than the $H_{(int)}$ to $H_{(ext)}$ interactions in cabazitaxel, this is not the case for the older generation taxanes.

Figure 2f depicts the general N interactions found on the Hirshfeld surfaces of the three taxanes. Although these cover 0.3% of the interactions for docetaxel and cabazitaxel alike, in the former they are completely accounted for by $N_{(int)}$ to $H_{(ext)}$ interactions, while in cabazitaxel only two thirds of these are attributed to $N_{(int)}$ to $H_{(ext)}$, with the other third being $N_{(int)}$ to $C_{(ext)}$ interactions.

The crystalline forms that afford a more accurate representation of the three-dimensional molecular arrangement of "free" cabazitaxel, without external influence from crystallized solvate molecules, are the anhydrous and hemihydrated forms. Although the presence of solvate molecules does alter the structure, the general trends in differences between cabazitaxel and its predecessors are still retained. ESI Table S2 summarises the distances and angles that characterise the orientation of the side chain with respect to the core molecule, in particular: the proximity of the t-butyl group of the side chain to the $C(CH_3)_2$ bridge on the core (distance **1**), the orientation of the side chain with respect to the $C(CH_3)_2$ bridge (improper torsion angle **2**), and the distance and orientation of the benzyl group of the core towards the side chain (distance **3** and improper torsion angle **4**).

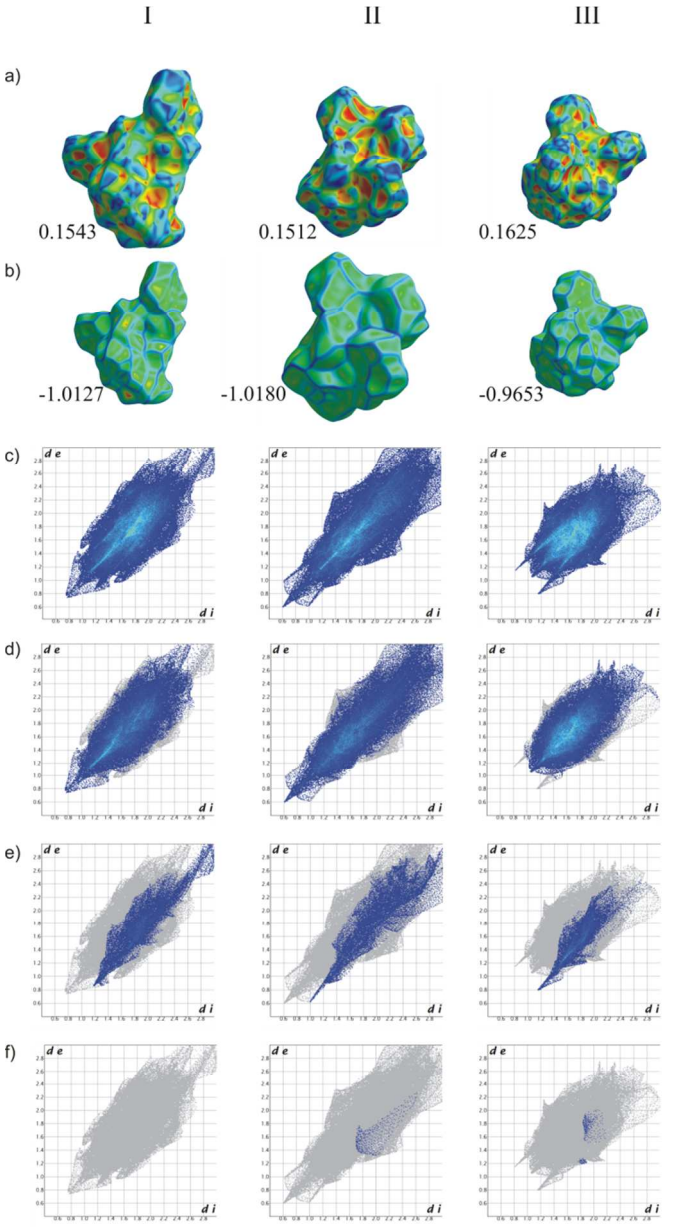

Fig. 2 Hirshfeld surfaces of the anhydrous forms of (I) paclitaxel, (II) docetaxel and (III) cabazitaxel, illustrating (a) the shape index, (b) curvedness, (c) global fingerprint plots, (d) $H_{(int)}$ to $H_{(ext)}$ interactions, (e) $O_{(int)}$ to $H_{(ext)}$ interactions, and (f) N interactions .

In comparison with the solvated forms of cabazitaxel, and with the anhydrous and hydrated forms of docetaxel and paclitaxel, these show a unique conformation of the side chain, as evidenced by values **2** and **4,** as well as in the closest C to C distance between the

t-butyl and $C(CH_3)_2$ moieties (distance **1**). In the literature, the distance between the side chain and the core C2 (distance **3**) is discussed to be directly related to the degree of reactivity for a specific conformation[19-21]. All the taxanes investigated so far show similar values for this distance, indicating that they have similar reactivity. Differences in the other values (**2**, **4** and **5**) suggest that these conformations may in fact be responsible for the altered and advantageous behaviour of cabazitaxel when compared to docetaxel and paclitaxel and that these conformational changes are retained in the solid state structure.

Although anhydrous and hydrated forms of the older-generation taxanes do adopt slightly altered arrangements compared to their respective solvates, remarkable differences exist between the conformations of the taxane molecules in these forms and those of anhydrous and hydrated cabazitaxel. Such differences also influence the sterical availability of groups for intermolecular interactions like hydrogen bonds or pi-stacking.

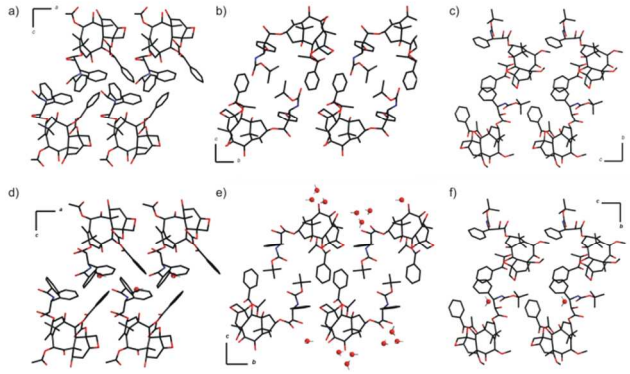

Fig. 3 Packing diagrams of the anhydrous forms of (a) paclitaxel, (b) docetaxel and (c) cabazitaxel, and of the hydrated forms of (d) paclitaxel, (e) docetaxel and (f) cabazitaxel. Hydrogen atoms on taxane molecules were omitted for clarity.

Fig. 3 shows marked differences in packing of cabazitaxel molecules in the crystalline solid compared to the corresponding anhydrous and hydrated forms of docetaxel and paclitaxel. Whereas in cabazitaxel the backbone phenyl ring and the phenyl/t-butyl groups face each other on opposite molecules (almost forming dimeric units), in paclitaxel and docetaxel the molecules are arranged in a zig-zag manner, adopting a much less compact shape. In both docetaxel and paclitaxel, the molecules are more stretched. Moreover, the t-butyl group in docetaxel is directed outwards and the phenyl rings are either further away from each other (within the same molecule) or above each other (in neighbouring molecules). Thus, the molecules are not grouped together but arranged in a manner where each molecule faces the same direction. In the paclitaxel structures the molecules only seem to be more compact, but in reality the phenyl rings of both backbone and side chain fit into the hollow parts of neighbouring molecules resulting in a clear zig-zag arrangement. The hydrates crystallise in very similar conformations to the anhydrous forms of their respective taxanes (Fig 3 and ESI Table S2).

In the distinct conformation of the cabazitaxel molecules the side chain and the phenyl group of the backbone adopt an almost perfect C shape conformation in which each end of the C faces the other end of the opposite molecule. This particular arrangement resembles the well-known bifurcated hydrogen bond motif between peptide sequences in which NH interacts with carbonyl O and vice-versa. This arrangement of molecules allows for tighter packing. In fact, when comparing the molecular volume of cabazitaxel (see ESI Table S1) and its crystal density with those of docetaxel and paclitaxel, cabazitaxel shows the smallest molecular volume (C: 1010.97Å, D: 1060.74Å, P: 1141.5Å) and its crystal density is the highest (C: 1.326g·cm^{-3}, D: 1.241g·cm^{-3}, P: 1.244g·cm^{-3})[11,12].

Comparison of the crystal structures of the anhydrous forms indicates that while the backbone remains unchanged for all three taxane molecules, the main difference lies in the orientation of the side chain (Fig. 1). Hirshfeld surface analysis revealed that O···H and H···H interactions are weaker in cabazitaxel than in paclitaxel and docetaxel, and this is therefore thought to be brought about majorly by the difference in side-chain conformation.

In discussing these structural features, we are not excluding the importance of the hydroxyl interaction between oxygen atoms O23 and O38 on docetaxel, or its implication in P-gp binding. The scope of this study was merely to draw attention to the presence of other previously unexploited effects and intermolecular attractions affecting the side chain conformation that might play a role in the permeability of cabazitaxel through the blood brain barrier, as well as its success in evading inhibition via P-gp.

Elucidation of the crystal structure of cabazitaxel in its anhydrous form, as well as in a series of solvated forms, is a major breakthrough for pharmaceutical materials science, offering insights into therapeutic data that have so far been difficult to explain. Analyses of shape and side-chain orientation, as well as exclusion of solid state effects due to solvent molecules, could only be afforded upon availability of the crystal structures of the drugs in their anhydrous and solvated or hydrated forms. The findings reported in this study will provide a platform for further development and exploitation of crystal structure towards the fine-tuning of the physical properties of active pharmaceutical ingredients.

Notes and references

[a] Crystal Engineering Laboratory, Department of Chemistry, University of Malta, Msida, MSD2080, Malta.
[b] School of Chemistry, Bedson Building, Newcastle University, Newcastle-upon-Tyne NE17RU, UK.

† Electronic Supplementary Information (ESI) available: Experimental procedures, characterization and related references. CCDC 940083-940087. For ESI and crystallographic data see DOI: 10.1039/c000000x/

1 R. Pazdur, A.P. Kudelka, J.J. Kavanagh, P.R. Cohen, and M.N. Raber, *Cancer Treat. Rev*. 1993, **19**, 351–386.
2 S.D. Baker, A. Sparreboom, and J. Verweij, *Clin. Pharmacokinet*., 2006, **45** (3), 235–252
3 A. Mendoza, Y. Ishihara and P.S. Baran, *Nature Chem.*, 2012, **4**, 21-25.
4 E.K. Rowinsky, *Ann. Rev. Med.*, 1997, **48**, 353–374.
5 D.G. Galsky, A. Dritselis, P. Kirkpatrick and W.K. Oh, *Nature Rev. Drug Discov.*, 2010, **9**, 677-678.
6 G.J.R. Zaman, *et al*., *Proc. Natl. Acad. Sci.*, 1994, **91**, 8822–8826.
7 T.W. Loo, and D.M. Clarke, *Biochem. Biophys. Res. Commun.*, 2005, **329**, 419-422.
8 J.S. de Bono, *et al*., *Lancet*, 2010, **376**, 1147-1154.
9 D.E. Oprea-Lager, *et al*., *Anticancer Research*, 2013, **33**, 387-391.
10 S. Lheureux and F. Joly, *Bull. Cancer*, 2012, **99**, 875-880.
11 A.C. Mita, R. Figlin and M.M. Mita, *Clin. Cancer Res.*, 2012, **18 (24)**, 6574-6579.
12 A. Heidenreich and D. Pfister, *European Oncology & Haematology* , 2012, **8(1)**, 42-45.
13 N. Agarwal, G. Sonpavde and C.N. Sternberg, *European Urology*, 2012, **61**, 950-960.
14 B. Kearns, M.L. Jones, M. Stevenson and C. Littlewood, *PharmacoEconomics*, 2013, 1-10.

15 M. Sun Jin, M.J. Oldham, Q. Zhang and J. Chen, *Nature*, 2012, **490**, 566-570.
16 L. Vella-Zarb, R.E. Dinnebier and U. Baisch, *Cryst. Growth Des*., 2013, **13**, 4402-4410.
17 L. Vella-Zarb, U. Baisch and R.E. Dinnebier, *J. Pharm. Sci*., 2013, **102(2)**, 674-683.
18 M. A. Spackman and J. J. McKinnon, *CrystEngComm*., 2002, **4**, 378–392; J.J. McKinnon, M.A. Spackman and A.S. Mitchell, *Acta Cryst.*, 2004, B**60**, 627-668; S.K. Wolff, D.J. Grimwood, J.J. McKinnon, D. Jayatilaka and M.A. Spackman, *CrystalExplorer, Version 3.1*, University of Western Australia, Perth, Australia, 2007.
19 E.M. Heider, J.K. Harper and D.M. Grant, *Phys. Chem. Chem. Phys.*, 2007, **9**, 6083-6097.
20 J.P. Snyder, J.H. Nettles, B. Cornett, K.H. Downing and E. Nogales, *Proc. Natl. Acad. Sci. U. S. A.*, 2001, **98**, 5312-5316.
21 M. Buchta, *et al*., *Z.Kristallogr.-New Cryst.Struct.*, 2006, **221**, 97-100.

